PLANCK 2015 RESULTS

S. HENROT-VERSILLE on behalf of the Planck collaboration
Laboratoire de l'Accélérateur Linéaire IN2P3-CNRS and Université de Paris-Sud XI, bat. 200 Centre scientique d'Orsay, F-91898 Orsay Cedex

The Planck 2015 cosmogical results are discussed with an emphasis on the improvements compared to the last data release, and on the methodology used to extract the parameters, both for the likelihood building and for the statistical method. As far as the base ΛCDM model is concerned, the implications of the cold dark matter density measurement in SUSY scenarios is illustrated. For the results on the extensions of ΛCDM, they are given for the neutrinos sector: the CMB being sensitive to the sum of the neutrino masses and to the effective number of relativistic degrees of freedom. Finally on the primordial gravitational waves side: implications in the strings parameters space derived from a limit set of the gravitational wave energy density is shown, as well as the limit on the tension over scalar ratio, r, coming from a combined analysis with BICEP.

1 Improvements, methodology and base ΛCDM results

The Planck mission has been launched in 2009 with the main objectives of measuring with an unprecedented accuracy the Cosmic Microwave Background (CMB) in an all-sky survey both in temperature and in polarisation. The satellite is composed of a 1.5m off-axis telescope at the focal plane of which are installed two instruments: the Low Frequency Instrument (LFI) measuring the CMB with HEMT in three frequency bands (30, 44 and 70 GHz), and the High Frequency Instrument (HFI) aiming at the measurement at higher frequencies (100, 143, 217, 353, 545 ad 857 GHz) with bolometers. Both instruments are sensitive to the polarisation: E-modes of the CMB are generated by Thomson scattering, while the B-modes are produced through two processes: the primordial tensor modes (i.e. primordial gravitational waves) and the lensing of the E-modes. While Planck was not designed to measure the B modes of the CMB, it does provide very important informations on the BB spectrum of the polarised dust (see section 2.2). A first round of results has been published in 2013 based on the first 14 months of the survey with the temperature data [1 2 3].

1.1 Improvements and spectra

The 2015 results [4] are based on the full Planck mission, including a first analysis of the polarisation data. Improvements have been made in the understanding of a remaining systematic effect due to the 4K cooler. The calibration discrepancy with the WMAP power spectra has been solved thanks to a better calibration procedure, and additionnal accuracy has been obtained in the beams characterisation. The main impact of these improvements is a reduction of both the statistical and systematical errors. In addition, while for the 2013 release, Planck did need the WMAP polarisation data at low multipole to constrain the cosmological parameters (mainly τ), the 2015 results are now fully based on Planck-only data (LFI+HFI). The resulting TT, TE and EE spectra are shown on figure 1, where the red line corresponds to the best fit cosmological

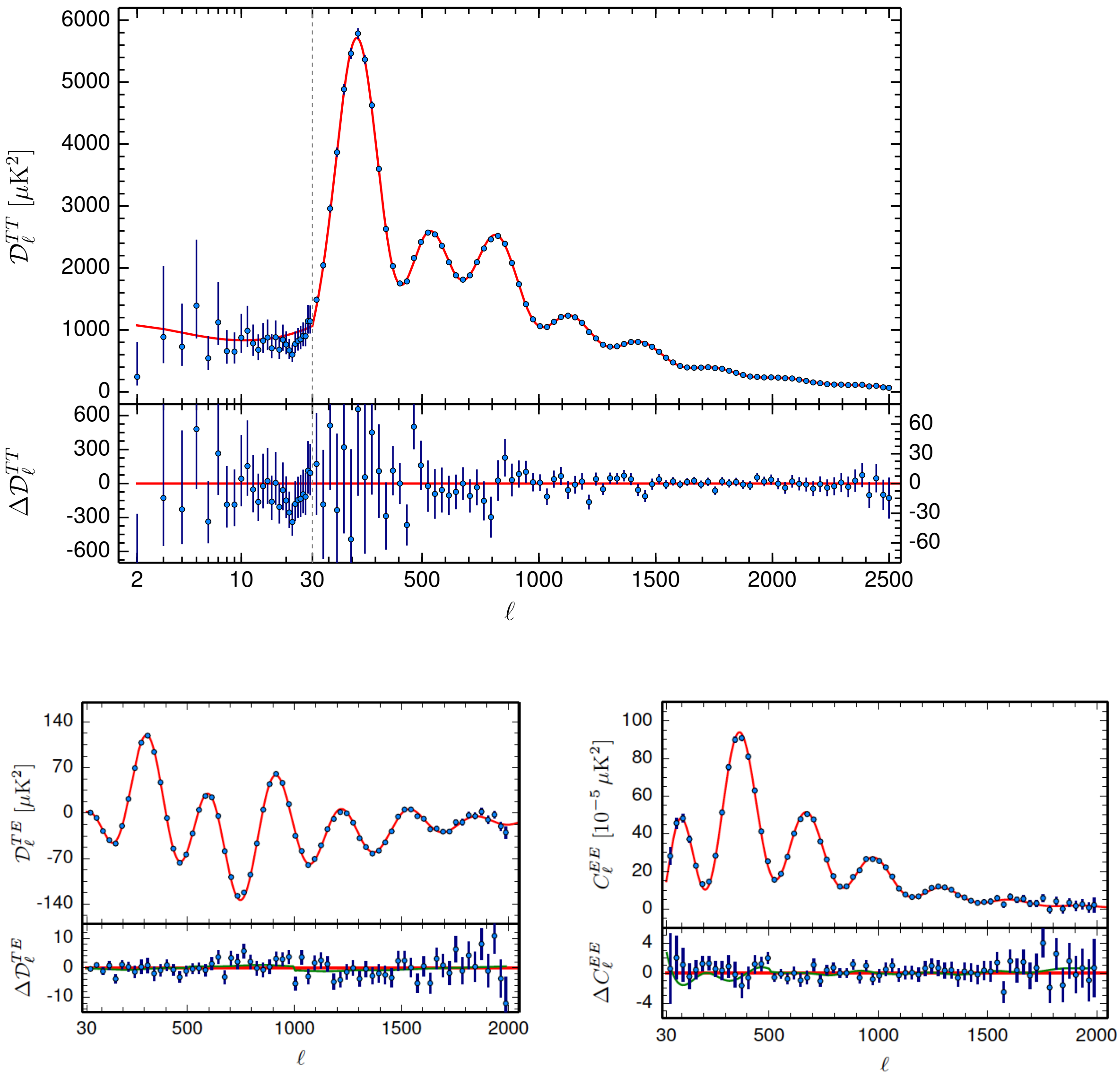

Figure 1 – Upper plot: temperature power spectrum, Lower plots: frequency averaged TE and EE spectra. The red lines correspond to the theoretical model for TT (upper), TE and EE (lower plots) computed using the Planck TT+lowP best fit corresponding to the upper plot.The error bars show $\pm 1\sigma$ errors.

parameters obtained with the temperature only data, showing that the polarisation spectra are already very well constrained by the cosmological information extracted from the temperature data.

1.2 Likelihood Building

To extract the cosmological parameters values from the Planck data, three likelihoods are used: a pixel-based one for the low multipoles (up to $\simeq 29$) that is built from low resolution maps of LFI (which is denoted lowP in the following), and a hybrid HFI likelihood using both a pixel based (for intermediate ℓ) and a spectra-based approach (for $\ell \geq 50$). This splitting is due to the expected statistical distribution of the C_ℓ which are assumed to be Gaussian for small angular scales, while the low ℓ regimes is driven by the cosmic variance. The high-ℓ likelihood can therefore be written under the form:

$$-2\ln\mathcal{L} = \sum_{\substack{X,Y=T,E \\ X',Y'=T,E}} \sum_{\substack{i,j=100.i\leq j \\ i',j'=100,i'\leq j'}}^{217} \sum_{\ell=\ell_{\min}^{X_iY_j}}^{\ell_{\max}^{X_iY_j}} \sum_{\ell'=\ell_{\min}^{X'_{i'}Y'_{j'}}}^{\ell_{\max}^{X'_{i'}Y'_{j'}}} \mathcal{R}_{\ell}^{X_iY_j} \left[\Sigma_{\ell\ell'}^{X_iY_j,X'_{i'}Y'_{j'}}\right]^{-1} \mathcal{R}_{\ell'}^{X'_{i'}Y'_{j'}}; \quad (1)$$

where the first sum is over the temperature/polarisation components while the second sum deals with the frequencies, $\mathcal{R} = C_\ell - \hat{C}_\ell$ denotes the residual of the estimated cross-power spectrum (C_ℓ) with respect to the model ($\hat{C}_\ell$) and Σ is the full covariance matrix. In $\mathcal{R}$ is incorporated the theoretical expected distribution of the anisotropies of the CMB, that is computed using a Boltzman code (see section 1.3), but also a parameterisation of the foregrounds (dust, synchrotron, point sources, cosmic infrared background ...). This is a matrix which size is of the order of 26000x26000 elements.

1.3 Statistical method and base ΛCDM results

The base ΛCDM model is described by 6 parameters: the baryon density of the Universe $\Omega_b h^2$, the Cold Dark Matter (CDM) density $\Omega_{cdm} h^2$, the characteristic angular size of the CMB fluctuations (θ_{MC}), the optical depth to reionization (τ) and the amplitude and spectral index of the primordial spectrum ($\ln(10^{10}A_s)$ and n_s). The sum of the neutrino masses is fixed and assumed to be 0.06eV. Two approaches can be followed to extract their values from the likelihood: using Monte Carlo Markov Chains followed by a Bayesian analysis or performing a profile likelihood analysis. Both methods have been tested, using a different Boltzman code for the evolution of the Universe, giving a completely independent cross-checks of the obtained results: for instance the profile method makes use of the CLASS software [5]. They both give similar results as it is shown on the first two columns of table 1: the small descrepancy observed for the characteristic size of the CMB fluctuations coming from a slightly different definition in the Boltzman codes.

Table 1: Mean values and errors obtained for the cosmological parameters within the ΛCDM scenario for the Planck temperature and LowP likelihood using the MCMC analysis (first column), and the profile likelihood method (second column). The third column gives the results for the combination of temperature and polarized Planck data with lensing [6] and external datasets (see text for details).

Parameter	PlanckTT+LowP (MCMC)	PlanckTT+LowP (Profiles)	TT,TE,EE+lowP +lensing+ext (MCMC)
$\Omega_b h^2$	0.02222 ± 0.00023	0.02227 ± 0.00023	0.02230 ± 0.00014
$\Omega_{cdm} h^2$	0.1197 ± 0.022	0.1198 ± 0.0022	0.1188 ± 0.0010
$100\theta_{MC}$ or $100\theta_0$	1.04085 ± 0.00047	1.04184 ± 0.00044	1.04093 ± 0.00030
τ	0.078 ± 0.019	0.082 ± 0.020	0.066 ± 0.012
$\ln(10^{10}A_s)$	3.089 ± 0.036	3.098 ± 0.037	3.064 ± 0.023
n_s	0.9655 ± 0.0062	0.9663 ± 0.0063	0.9667 ± 0.0040

The parameters values and their errors are given in the last column of table 1 when the Planck likelihood described previously is combined with the lensing information and external datasets: the Baryon Acoustic Oscillations measurements [7], the Type Ia supernovae from the Joint Light curve Analysis [8], and the Hubble constant measurement as explained in [4].

1.4 CDM and SUSY

As an illustration of the implications of the CDM density measurement of Planck, figure 2 shows the favored area (the reddish, the more favored is the region) in the (M_2, M_1) and (μ, M_1) parameters spaces of a TeV-scale 13 parameters MSSM (Minimal SuperSymmetric Model)

SUSY model, where the minimum value of all squarks (except the stop) masses has been set to 2 TeV in order to be above the LHC present limits, M_3 is fixed to 2 TeV and $A_b = 0$. This SFitter[9] analysis[10] has been performed using a combination of cosmological and particle physics measurements (namely $\Omega_{cdm}h^2$ from Planck[3], the Higgs boson mass[11], the branching ratios of rare B decay[12], the top mass[13] and the anomalous moment of the muon[14] and the Xenon limit[15]). The pattern of the favored regions is mainly driven by the Higgs mass and the CDM measurement through the dark matter annihilations channels. Given the theoretical error on $\Omega_{cdm}h^2$ due to the extrapolation of the SUSY branching ratios which is of the order of 0.012 (to be compared to the statistical error from table 1), those analyses are already limited by the theory error.

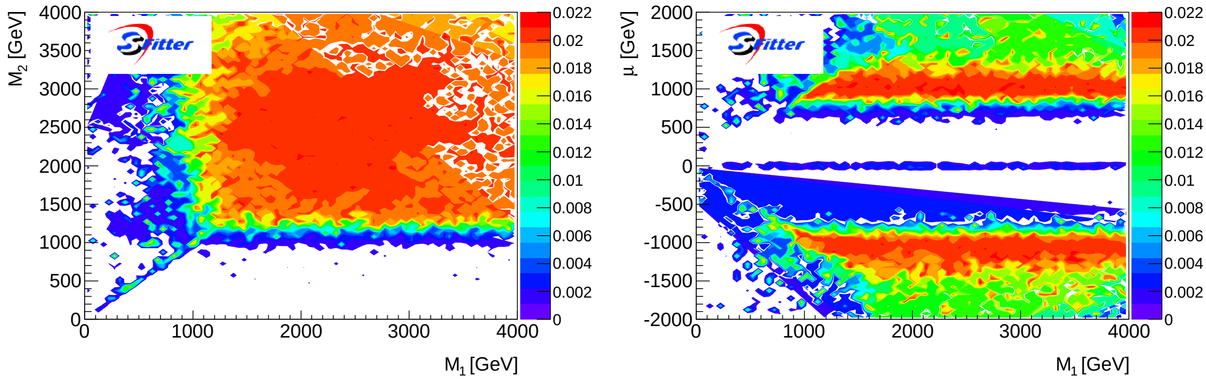

Figure 2 – Profile likelihood projection onto the (M_1, M_2) plane (left) and the (M_1, μ) plane (right).

2 ΛCDM extensions

A very complete set of ΛCDM extensions has been explored by the Planck collaboration[4]. This talk concentrates on the neutrino and the primordial gravitational wave (GW) background sectors.

2.1 The neutrino sector

The CMB is sensitive to the sum of the neutrino masses, impacting the first acoustic peak and the shape of the spectrum on small scales. The combined temperature information with LowP, the Planck lensing, and the external dataset, the obtained limit reaches $\sum(m_\nu) < 0.23$ eV at 95% CL. Combining those measurements with to-come oscillations results will probably allow to test the hierarchy in the near future.

CMB can also constrain the effective number of relativistic degrees of freedom $N_{\rm eff}$. Under the assumption that only the photons and the standard light neutrinos contribute to the radiation, this parameter is the effective number of neutrinos and is expected to be 3.046[16]. Any deviation from this value can be attributed to either sterile neutrino, axions[17,18], decay of non-relativistic matter[19], extra dimensions[20,21,22], early dark energy[23], asymmetric dark matter[24], or leptonic asymmetry[25], or even primordial gravitational waves[26]. The results are summarized in table 2 for temperature and polarisation, with and without BAO data. Within the obtained error, one cannot conclude of a convincing evidence for any extra relativistic component.

2.2 The primordial gravitational waves

Inflation predicts the existence of a background of gravitational waves (GW) or tensor modes fluctuations[27,28,29,30]. From the observations of the CMB, since those GW contribute to the

Table 2: N_{eff} limit at 95%CL obtained for different combinations of likelihoods including the Planck 2015 temperature (TT), and low multipoles polarisation (lowP). Illustrations of the impact of the use of high multipoles polarisation data (TE and EE) and BAO are also given.

3.13 ± 0.32	Planck TT +lowP
3.15 ± 0.23	Planck TT +lowP +BAO
2.99 ± 0.20	Planck TT,TE,EE +lowP
3.04 ± 0.18	Planck TT,TE,EE +lowP +BAO

anisotropies (both in temperature and linear polarisation), one can deduce constraints on related parameters such as their energy density, $\Omega_{GW}h^2$, and the tensor to scalar ratio, r .

from N_{eff}

Using the N_{eff} results, one can set a limit on the gravitational wave energy density through the relation [31,16]:

$$\Omega_{GW}h^2 \leq \frac{7}{8}(\frac{4}{11})^{4/3}(N_{eff} - 3.046)\Omega_\gamma \ , \qquad (2)$$

for which an analysis has been performed using profile likelihoods [32] with the 2013 Planck data (combined with the Wmap data at low ℓ, the BAO and the Lensing) and leads to $\Omega_{GW}h^2 <$ 3.8 10^{-6}. Assuming the GW can be attributed to a network of cosmic strings, this result can be interpreted as exclusions limits in the strings parameters space as shown in figure 3 where is shown the new limit obtained for the small loop regime (with $p = 10^{-3}$) in the loop size vs. string tension space, pushing further the previous constraints. If the size of the loops is determined by gravitational back-reaction, string tension values greater than $\sim 4 \times 10^{-9}$ are excluded for a reconnection probability of 10^{-3}.

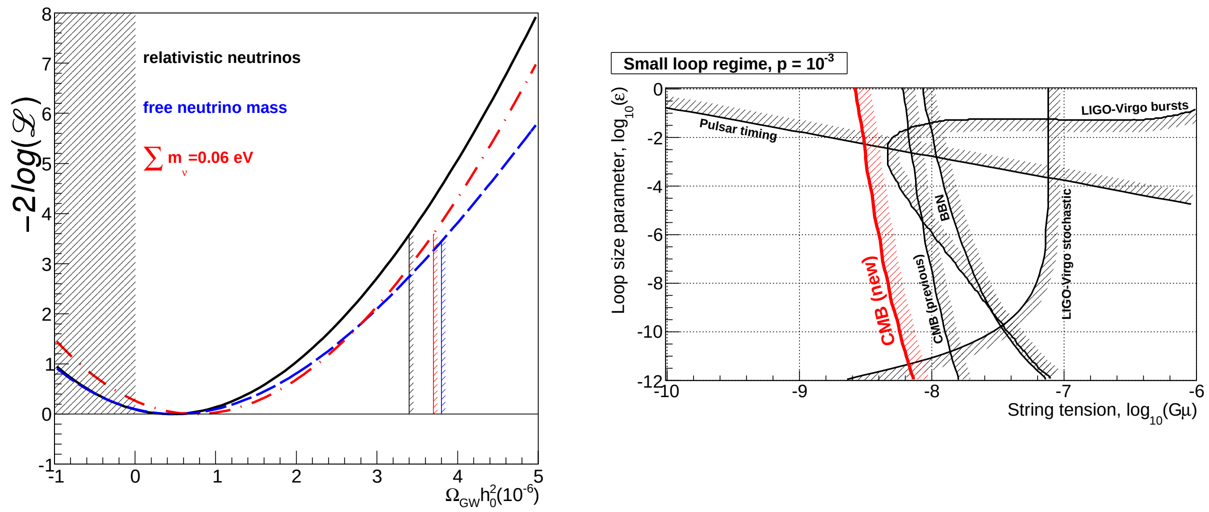

Figure 3 – Left hand side: $\Omega_{GW}h^2$ profile likelihood obtained with the full Planck+WP+highL+BAO+Lensing 2013 data set in three neutrino models: when they are considered to be massless (in black full lines), when $\sum m_\nu = 0.03$ eV (in red dashed and dotted lines) and when the neutrino mass is free to vary in the fit (blue dashed lines). Right hand side: constraints on cosmic string parameters $(G\mu, \epsilon)$ assuming the loops are small and fixing $p = 10^{-3}$. The new constraints are compared to previous ones [26].

from B modes

With the 2013 release, Planck published the best limit on the tensor modes using CMB alone [3] with $r < 0.11$ at 95%CL. In 2014, BICEP2, a low angular resolution experiment operating at the South Pole from 2010 and 2012, published [33] a B-mode excess measurement above the $r = 0$ lensed ΛCDM expectation for $0 \leq \ell \leq 150$. In 2014, Planck released two papers: one on the structure of the dust polarisation [34] and one on the frequency dependence [35] of this emission relevant to CMB studies. Consequently, a joint analysis [36] of both datasets has been performed showing that no significant evidence for primordial gravitational waves was found. An upper limit on the tension over scalar ratio has been deduced and gives $r < 0.12$ at 95%CL.

3 Conclusions

The Planck 2014 release includes a first release of all sky polarisation data from LFI (30, 44, 70 GHz) and HFI (353 GHz). The high quality data (CMB and Lensing) confirm the ΛCDM base model with an unprecedented accuracy and permit to test its extensions. The next Planck challenge is the release of cleaned HFI polarised data at 100, 143, and 217 GHz.

References

1. P. A. R. Ade *et al.* [Planck Collaboration], Astron. Astrophys. **571**, A15 (2014)
2. P. A. R. Ade *et al.* [Planck Collaboration], Astron. Astrophys. **571**, A17 (2014)
3. P. A. R. Ade *et al.* [Planck Collaboration], Astron. Astrophys. **571**, A16 (2014)
4. P. A. R. Ade *et al.* [Planck Collaboration], arXiv:1502.01589 [astro-ph.CO].
5. Lesgourgues, J. 2011, arXiv:1104.2932
6. P. A. R. Ade *et al.* [Planck Collaboration], arXiv:1502.01591 [astro-ph.CO].
7. Beutler, F., Blake, C., Colless, M., et al. 2011, Mon. Not. Roy. Astron. Soc. 416, 3017 Anderson, L., Aubourg, E., Bailey, S., et al. 2012, Mon. Not. Roy. Astron. Soc. 427, 3435 A. J. Ross, L. Samushia, C. Howlett, W. J. Percival, A. Burden and M. Manera, Mon. Not. Roy. Astron. Soc. **449**, 835 (2015)
8. Betoule, M., Marriner, J., Regnault, N., et al. 2013, Astronomy and Astrophysics, 552, A124
9. R. Lafaye, T. Plehn and D. Zerwas, arXiv:hep-ph/0404282;
   R. Lafaye, T. Plehn, M. Rauch and D. Zerwas, Eur. Phys. J. C **54**, 617 (2008).
10. S. Henrot-Versillé, R. Lafaye, T. Plehn, M. Rauch, D. Zerwas, S. Plaszczynski, B. Rouill d'Orfeuil and M. Spinelli, Phys. Rev. D **89**, no. 5, 055017 (2014)
11. ATLAS Collaboration, Science **338**, 1576 (2012).
12. R. Aaij *et al.* [LHCb Collaboration], Phys. Rev. Lett. **110**, 021801 (2013), CMS Collaboration, Phys. Rev. Lett. **111**, 101804 (2013), Particle Data Group http://pdg.lbl.gov/2012/reviews/rpp2012-rev-b-meson-prod-decay.pdf
13. Particle Data Group:
    http://pdg.lbl.gov/2012/reviews/rpp2012-rev-standard-model.pdf
14. Particle Data Group:
    http://pdg.lbl.gov/2012/reviews/rpp2012-rev-g-2-muon-anom-mag-moment.pdf
15. E. Aprile *et al.* [XENON100 Collaboration], Phys. Rev. Lett. **107**, 131302 (2011);
    E. Aprile *et al.* [XENON100 Collaboration], Phys. Rev. Lett. **109**, 181301 (2012)
16. Mangano G, Miele G, Pastor S, Pinto T, Pisanti O *et al.* 2005 *Nucl.Phys.* **B729** 221–234
17. Melchiorri A, Mena O and Slosar A 2007 *Phys.Rev.* **D76** 041303
18. Hannestad S, Mirizzi A, Raffelt G G and Wong Y Y 2010 *JCAP* **1008** 001
19. Fischler W and Meyers J 2011 *Phys.Rev.* **D83** 063520
20. Binetruy P, Deffayet C, Ellwanger U and Langlois D 2000 *Phys.Lett.* **B477** 285–291
21. Shiromizu T, Maeda K i and Sasaki M 2000 *Phys.Rev.* **D62** 024012

22. Flambaum V and Shuryak E 2006 *Europhys.Lett.* **74** 813–816
23. Calabrese E, Huterer D, Linder E V, Melchiorri A and Pagano L 2011 *Phys.Rev.* **D83** 123504
24. Blennow M, Fernandez-Martinez E, Mena O, Redondo J and Serra P 2012 *JCAP* **1207** 022
25. Caramete A and Popa L 2014 *JCAP* **1402** 012
26. Smith T L, Pierpaoli E and Kamionkowski M 2006 *Phys.Rev.Lett.* **97** 021301
    Sendra I and Smith T L 2012 *Phys.Rev.* **D85** 123002
27. Grishchuk L 1975 *Sov. Phys. JETP* **40** 409–415
28. Starobinski A 1979 *JETP Lett.* **30** 682–686
29. Bar-Kana R 1994 *Phys.Rev.* **D50** 1157–1160 (*Preprint*
30. Easther R, Giblin John T J and Lim E A 2007 *Phys.Rev.Lett.* **99** 221301 (*Preprint*
31. Maggiore M 2000 *Phys.Rept.* **331** 283–367
32. Henrot-Versillé, S., Robinet, F., Leroy, N., et al. 2015, Classical and Quantum Gravity, 32, 045003
33. P. A. R. Ade *et al.* [BICEP2 Collaboration], Astrophys. J. **792**, 62 (2014) [arXiv:1403.4302 [astro-ph.CO]].
34. Planck Collaboration, Ade, P. A. R., Aghanim, N., et al. 2015, Astronomy and Astrophysics, 576, A104
35. Planck Collaboration, Ade, P. A. R., Alves, M. I. R., et al. 2015, Astronomy and Astrophysics,, 576, A107
36. P. A. R. Ade *et al.* [BICEP2 and Planck Collaborations], Phys. Rev. Lett. **114**, no. 10, 101301 (2015) [arXiv:1502.00612 [astro-ph.CO]].